Quantitative Analysis of Retinal Ganglion Cell (RGC) Loss in Aging DBA/2NNia Glaucomatous Mice: Comparison with RGC Loss in Aging C57/BL6 Mice

John Danias,[1,2] *Kevin C. Lee,*[1,2] *Maria-Florencia Zamora,*[1,2] *Bin Chen,*[1] *Fran Shen,*[1] *Theodoros Filippopoulos,*[1] *Yanling Su,*[1] *David Goldblum,*[1] *Steven M. Podos,*[1] *and Thom Mittag*[1]

Purpose. To quantify the extent and pattern of retinal ganglion cell (RGC) loss in the DBA2/NNia glaucomatous mouse strain as a function of age and compare it with ganglion cell loss in a nonglaucomatous strain.

Methods. All the ganglion cells in retinas of DBA/2NNia and C57/BL6 mice of various ages (five eyes per age group in 3-month intervals from 3 to 18 months of age) were counted. A novel counting method that does not rely on sampling and that uses retrograde labeling of RGCs with Fluorogold (Fluorochrome; Englewood, CO) was used. RGC loss in the glaucomatous DBA/2NNia mouse strain was contrasted to RGC loss in C57 mice at the same ages. The total number of Fluorogold-labeled cells per retina was compared within and among the two strains as a function of age. In addition, RGC density maps were constructed for each retina, and the range of densities for each age group was compared within and among the two strains. IOP in awake, nonsedated DBA/2NNia mice was measured with a rebound tonometer.

Results. RGC loss started between 12 and 15 months of age in C57 mice and led to an approximate 46% reduction by 18 months of age. The rate of loss was best approximated by a second-order polynomial curve. In comparison, DBA/2NNia mice also began showing RGC loss at approximately 12 months of age, but it proceeded at a much faster rate, with approximately 64% of their RGCs dying by the 15th month of age but little additional loss thereafter. RGC loss in the DBA animals had a focal pattern that appeared more patchy and showed greater variability than the age-related loss in C57 mice, which was more diffuse. IOP and total retinal area in DBA/2NNia mice began to increase at approximately 6 months of age. IOP normalized after the 12th month of age.

Conclusions. Age-related RGC loss of up to 50% can occur in the C57 mouse by 18 months of age. The loss does not proceed linearly with age, as is often assumed, and differs both in extent and locational pattern from pathologic RGC loss secondary to glaucoma in DBA/2NNia mouse retinas. (*Invest Ophthalmol Vis Sci.* 2003;44:5151–5162) DOI:10.1167/iovs.02-1101

The DBA/2 mouse strain represents an animal model of human glaucoma. In this mouse strain, anterior segment abnormalities develop, that include iris atrophy, pigment dispersion, and peripheral anterior synechiae that are associated with development of elevated intraocular pressure (IOP) starting at approximately 6 months of age.[1,2] These pathologic changes are progressive and affect, to some degree, almost all the mice by 9 months of age. Histologic study of the eyes at later ages has shown thinning of the nerve fiber layer, retinal ganglion cell (RGC) loss, and optic nerve atrophy.[1–3] The genetics associated with this secondary glaucoma have been worked out and extended to the discovery of similar genetic abnormalities associated with some cases of human pigmentary glaucoma.[4]

In our previous study on the DBA/2 NNia mouse substrain we documented electroretinographic abnormalities and significant thinning of all retinal layers compared with C57 mice, which began at approximately 7 months of age, well before RGC death.[3] The need to compare progressive RGC loss with age in DBA/2 mice in parallel with another nonglaucomatous strain arises because many studies indicate that a progressive loss of certain groups of neurons occurs naturally with increasing age (reviewed in Esiri et al.[5]). It has been hypothesized that these changes account for some of the functional deficits of aging.[6] In the retina, age-related progressive neuronal loss has been reported in the past.[7–10] However, the time course of RGC loss has not been adequately investigated.

Therefore, in the present study, we set out to quantify RGC loss occurring in a DBA/2 mouse substrain in which secondary glaucoma and pathologic RGC loss spontaneously develop,[1,2] in parallel with RGC loss that occurs in same-age C57 mice. We used the C57/BL6 strain as a reference strain not only because it is in common use by many other investigators but also because it has been reported that age-related losses in this strain can be rather large, with more than 70% of particular types of neurons being lost by 24 months of age.[11] Despite evidence to the contrary,[11] it is often assumed that the loss of neurons proceeds linearly with age. The present study attempts to quantify RGC loss accurately by counting and mapping the RGCs in the entire retina of DBA/2NNia and C57BL/6 mice over the age range of 3 to 18 months.

Materials and Methods

Animals

DBA/2NNia mice (raised at Mount Sinai School of Medicine from founding stock supplied by William G. Sheldon from the National

From the [1]Department of Ophthalmology, Mount Sinai School of Medicine, New York, New York.

[2]Contributed equally to the work and therefore should be considered equivalent senior authors.

Supported by National Eye Institute Grants K08-EY00390, R01-EY11649, R01-EY01867, R03-EY13732; an unrestricted research grant, a Senior Fellowship award (TM), and a Medical Student Eye Research Fellowship grant (KCL) from Research to Prevent Blindness; the May and Samuel Rudin Family Foundation Inc.; and the Swiss National Foundation and M+W Lichtenstein Stiftung.

Submitted for publication October 29, 2002; revised April 1, April 29, and June 5, 2003; accepted June 16, 2003.

Disclosure: **J. Danias** (P); **K.C. Lee**, None; **M.-F. Zamora**, None; **B. Chen**, None; **F. Shen**, None; **T. Filippopoulos**, None; **Y. Su**, None; **D. Goldblum**, None; **S.M. Podos**, None; **T. Mittag** (P)

The publication costs of this article were defrayed in part by page charge payment. This article must therefore be marked "*advertisement*" in accordance with 18 U.S.C. §1734 solely to indicate this fact.

Corresponding author: John Danias, Department of Ophthalmology, The Mount Sinai Medical Center, 1 Gustave L Levy Place, New York, NY 10029; john.danias@mssm.edu.

Center for Toxicological Research, Jefferson, AR) and age-matched C57/BL6 mice (Harlan, provided by the National Institute of Aging, Bethesda, MD) at 3, 6, 9, 12, 15, and 18 months of age (four mice per age group) were used for the experiments. Animals were housed in covered cages and were fed a standard rodent diet (Laboratory Diet 5001; Purina Mills) and fresh water ad libitum. The temperature was kept constant at 22°C. A 12-hour light–dark cycle was maintained. All mice were handled according to the ARVO Statement for the Use of Animals in Ophthalmic and Vision Research, and the experimental protocol was approved by the Institutional Animal Care and Use committee of Mount Sinai School of Medicine.

RGC Labeling

Mice were anesthetized by intraperitoneal or intramuscular administration of a mixture of xylazine (10.8 mg/kg), acepromazine (1.2 mg/kg), and ketamine (54.0 mg/kg). The skin over the cranium was incised, and the scalp was exposed. Holes approximately 2 mm in diameter were drilled in the skull 4 mm posterior to bregma, 1 mm lateral to the midline, with a dentist's drill (Dremel, Racine, WI) on both sides of the midline raphe. These positions correspond to the superior colliculi as determined from a stereotactic mouse brain atlas.[12] The superior colliculi were exposed by gentle aspiration of the overlying occipital cortex. A piece of Gelfoam (Pharmacia & Upjohn, Kalamazoo, MI) soaked in a 5% solution of the neurotracer dye Fluorogold (Fluorochrome, Denver, CO) was directly applied to each superior colliculus. Skull openings were then sealed with a petrolatum-based antibiotic ointment. The overlying skin was sutured and antibiotic ointment applied externally.

Retinal Flatmount Preparation

Five to 7 days after the application of Fluorogold (time enough to allow retrograde uptake of the dye and labeling of the RGC somata), mice were killed by transcardial perfusion with 4% buffered paraformaldehyde (Sigma-Aldrich, St. Louis, MO) while under the same anesthesia as that used for RGC labeling. Eyes were immediately enucleated, and the retinas were detached at the ora serrata and cut with a trephine around the optic nerve head. Eight radial relaxing incisions were made and the retinas prepared as flattened wholemounts on silane-coated microscope slides (Sigma-Aldrich) as previously described,[13] using the caruncle as the orientation landmark.

Imaging

Imaging of the Fluorogold-labeled retinas was performed with a digital camera (Pixera, Los Gatos, CA) and a fluorescence microscope with a 20× objective (Carl Zeiss Meditec, Oberkochen, Germany) equipped with a motorized stage (Ludl, Hawthorne, NY). The entire retina was imaged by adjacent, nonoverlapping frames captured in a raster pattern (approximately 250 frames per retina) each covering an area of 0.089 mm^2 at a resolution of 3.44 pixels/μm^2. Images were saved on a CD for further computer analysis. The final magnification of each frame on which automated counting was performed was approximately 800.

We started the experiment with four mice per group. However, in some of the older age groups one of the animals died during Fluorogold labeling. In addition, some of the retinas could not be used for automated counting, because they were either damaged during flatmounting or were not planar enough to be fully imaged. To limit the number of retinas analyzed to a reasonable number and keep the group size the same, we randomly selected five retinas per group that were suitable for complete imaging in 6 of the 12 groups where additional usable retinas were available. No selection for pairing, disease, or gender, was performed.

RGC Counting

Computer-aided counts were performed with commercially available imaging software, as previously described.[13] Images were initially converted to gray scale with customized image-analysis software (Photoshop, ver. 6.0; Adobe Systems, Inc., San Jose, CA) script. ImageTool, ver. 3.0 (University of Texas Health Science Center San Antonio [UTHSCSA], San Antonio, TX) was then used to obtain a rapid count of all RGCs in each frame. A size threshold criterion allows for discrimination between fluorescent cells and background and noise, and was estimated as previously described.[13]

Validation of Counting Method

Automated counting of RGCs was adapted from the previously published procedure for the rat retina.[13] The algorithm for counting mouse RGCs by this procedure was established by experiment. Counts obtained by the automated computer-aided method were compared with manual counts of the same frame performed by three independent, masked operators. Twenty-seven full frames covering the density range of 100 to 700 RGCs per frame (densities ranging from ~1100 to ~8000 RGCs/mm^2) from randomly selected retinas of DBA/2NNia mice between the ages of 3 and 15 months were counted, and the counts were correlated with the automated counts to establish the validity of the method.

Area Calculations and Density Maps

Composite maps of each retina were generated using the Image Tool (ver. 3.0), image-analysis program from the individual color frames. These maps were then used to determine the area within each frame occupied by retina, by interactively drawing around the circumference of the whole retina and then thresholding the area of interest. The density of each frame was calculated by dividing the number of cells with the frame area. A value between 0 and 255 was assigned to each density level in a linear manner. These values were used to generate gray-scale maps of each retina as a composite of the densities of all the frames.

Statistical Analysis

Results were recorded in spreadsheets (Excel 2000; Microsoft Corp, Redmond, WA) and evaluated with parametric tests. General linear model two-way ANOVA was used to compare means of RGC counts among strains and ages. One-way ANOVA was used to compare animals of different ages within the same strain. Post hoc analysis was performed with the Bonferroni test to determine which mean counts in an age group differed from the counts in other age groups. Student's *t*-test was used to compare animals of the two different strains at each age point. The level of significance was $P < 0.05$ (two-tailed test) in all statistical testing. Analyses were performed on computer (NCSS software, Kaysville, UT).

IOP Measurements

IOP was measured noninvasively in another group of awake, nonsedated DBA/2NNia mice of various ages (four to eight eyes at each age point) with a rebound tonometer.[14] Eyes were anesthetized with tetracaine 0.5% before IOP measurements. Animals were restrained in a custom-made device that allows measurement of IOP without causing an increase in intrathoracic pressure. Five measurements were taken from each eye and averaged.

Results

Validation of the Automated Counting Method

A representative frame from a mouse retina (Fig. 1A) and the binary image (Fig. 1B) to which it is converted for automated counting is shown in Figure 1.

RGC counts obtained using this automated quantification method have a strong linear correlation ($R^2 = 0.954$) with manual counts (Fig. 2) over the range of densities (100–700 cells/frame at this magnification) found in mouse retinas. Thus, application of the counting algorithm derived in Figure 2 allows for accurate estimates of the actual number of RGCs.

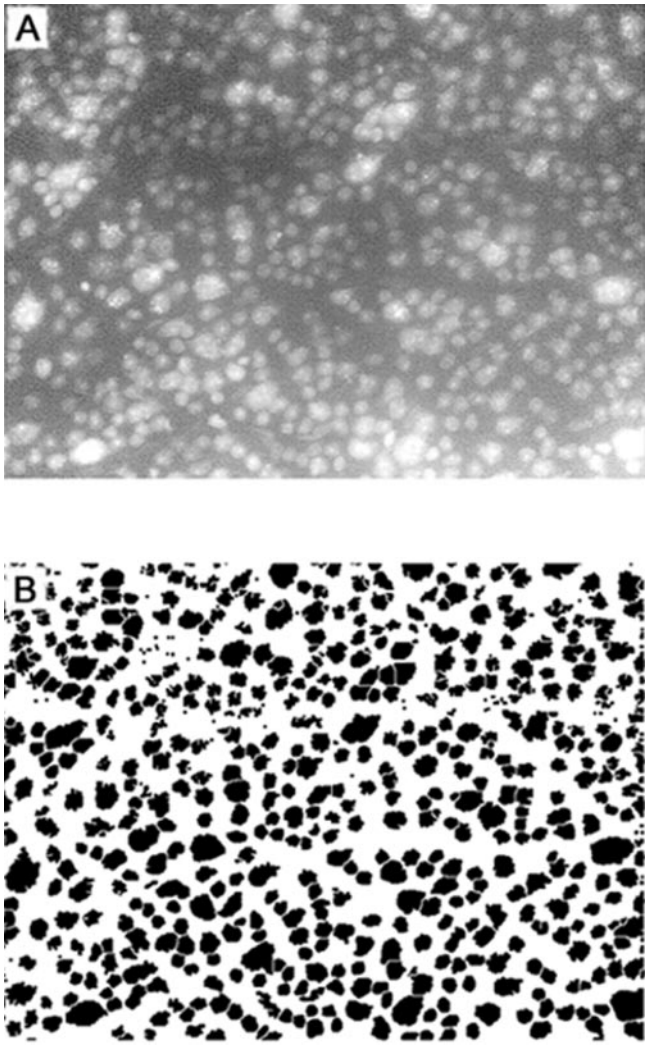

FIGURE 1. Representative image from a flatmounted mouse retina (**A**) and corresponding binary image used for automated RGC counting (**B**).

IOP Measurements in DBA2/NNia Mice

IOP in DBA/2NNia mice of various ages from 3 to 15 months is shown in Figure 3. IOP began to increase in some eyes at approximately 6 months of age. However, not all eyes had elevated IOP by 6 or 9 months. IOP started to decrease in all eyes to early levels (3 months of age) after the 12th month and remained in this range up to the 18th month.

Comparison of RGC Counts and Total Retinal Area between C57/BL6 and DBA/2NNia Mice

Mean RGC counts, mean retinal areas, and average retinal density per retina for each age group within each strain are presented in Table 1. RGC counts of the two strains differ significantly ($P < 0.022$) when compared in a two way (by strain, by age) ANOVA. The age effect is also statistically significant ($P < 0.000001$), as is the interaction of strain with age ($P < 0.032$). In addition, total retinal areas differ ($P < 0.00006$) between the two strains when compared in a two-way (by strain, by age) ANOVA. The age effect is again statistically significant ($P < 0.000009$), as is the interaction of strain with age ($P < 0.02$).

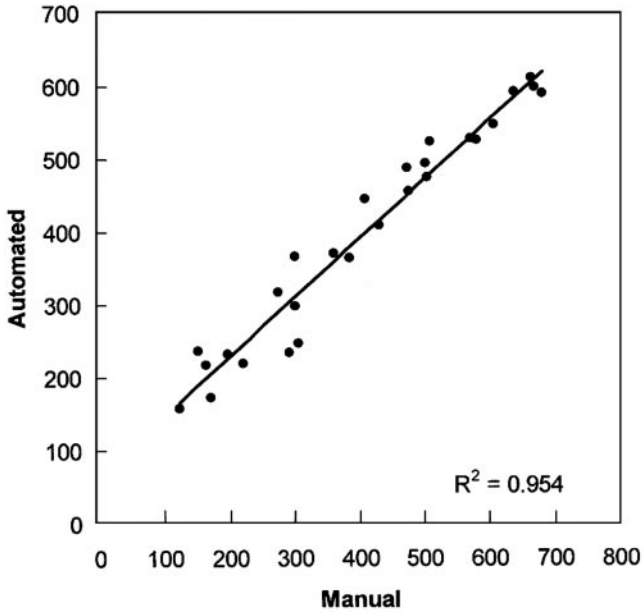

FIGURE 2. Manual versus automated counting of RGCs over the range of approximately 1100–8000 cells/mm^2. Best-fit linear regression correlation coefficient (R^2) is indicated.

RGC Counts and Total Retinal Area in C57/BL6 Retinas

RGC counts of C57/BL6 mice of ages 3 to 18 months are shown in Figure 4. Analysis of variance (ANOVA) among the various groups, shows a statistically significant difference ($P < 0.00045$). C57 mice of ages 3, 6, and 9 months had a similar mean number of RGCs. Retinas of 12- and 15 month-old C57 animals demonstrated a mean decline of approximately 18% in cell count from that in younger mice, which did not reach a significant difference from the RGC counts of younger animals ($P > 0.05$, Bonferroni multiple comparison post hoc analysis). By 18 months of age, C57 mice had lost up to approximately 46% of their RGCs, a significant difference from all other groups ($P < 0.05$, Bonferroni multiple comparison post hoc analysis). The age-dependent loss of RGC in C57 mice appeared to be diffuse. The standard error of counts is 7944, 7419, and 3550 for the 12-, 15-, and 18 month-old groups, respectively. All the count data taken together indicate that

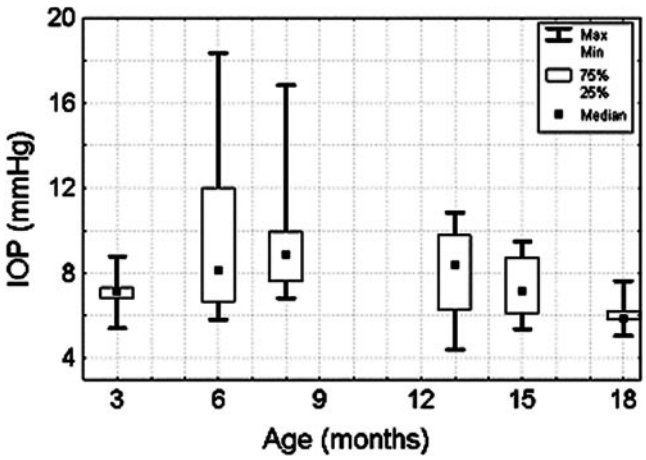

FIGURE 3. IOP measurement in DBA/2NNia mice of various ages (minimum of four eyes per age group).

TABLE 1. Mean RGC Counts, Retinal Area and Average RGC Density for Each Age Group in Both Strains

Strain	Age (mo)	RGC Count (n)	Retinal Area (mm^2)	RGC Density per Retina (RGC/mm^2)
DBA2/NNia	3	89,492 ± 5,746.0	16.59 ± 0.17	5,396 ± 362
	6	73,834 ± 4,698.8	15.33 ± 0.31	4,805 ± 243
	9	86,363 ± 9,995.3	19.46 ± 0.82	4,403 ± 417
	12	72,322 ± 5,192.7	18.69 ± 0.50	3,882 ± 295
	15	30,769 ± 8,877.0	19.32 ± 0.32	1,583 ± 440
	18	25,106 ± 13,087.3	19.22 ± 0.65	1,248 ± 605
C57/BL6	3	84,027 ± 2,171.6	15.97 ± 0.37	5,268 ± 136
	6	83,925 ± 5,549.8	16.82 ± 0.26	4,980 ± 279
	9	85,168 ± 6,118.7	17.14 ± 0.44	4,954 ± 280
	12	69,824 ± 7,943.6	16.43 ± 0.85	4,212 ± 323
	15	69,002 ± 7,419.0	17.61 ± 0.59	3,916 ± 389
	18	45,890 ± 3,549.8	16.90 ± 0.17	2,724 ± 232

Density was calculated as total RGC count divided by total retinal area. Data are expressed as the mean ± SEM.

loss of RGCs with age appears to fit better a second-order polynomial decay curve (Fig. 3, dotted line; $R^2 = 0.55$) than a linear relationship ($R^2 = 0.47$) in C57 mice.

Total retinal area did not change significantly in C57/BL6 mice from 3 to 18 months of age (one-way ANOVA, $P = 0.30$, power 0.37).

RGC Counts and Total Retinal Area in DBA Mice

RGC counts in retinas of DBA/2NNia mice 3 to 18 months of age are shown in Figure 5. At the ages of 3, 6, and 9 months, retinas had counts between 73,834 and 89,492 RGCs. Eyes of 12-month-old animals began to show a very small decline in total RGCs, with an average of 72,339 RGCs, which was not significantly different from earlier time points. A much greater decline was evident in 15-month-old DBA mice, which had an average of 30,769 RGCs per eye. This represented an approximate 64% decrease in the number of cells compared with retinas of younger eyes and was statistically significant ($P < 0.05$, Bonferroni multiple comparison post hoc analysis). By 18 months, DBA retinas had an approximate 71% decline in the number of RCGs compared with the 3-month-old eyes ($P < 0.05$, Bonferroni multiple comparison post hoc analysis). However, the loss of RGCs at 18 months was not significantly greater when compared with that in 15-month-old retinas. In the groups of mice showing loss of RGCs there was an increasing variability between individual retinas, as indicated by the increasing SEMs for groups at 12, 15, and 18 months of 5,193, 8,877, and 13,087, respectively.

Total retinal area appeared to be different among DBA/2NNia mice of ages between 3 and 18 months (one-way ANOVA, $P = 0.000002$). This difference was attributable to an increase in the area in the 9-, 12-, 15-, and 18-month retinas compared with that of 3- and 6-month-old retinas (see Table 1, $P < 0.05$, Bonferroni multiple comparison post hoc analysis).

Density Maps and Pattern of RGC Loss

Retinas of both C57 and DBA mice showed loss of RGCs at 15 and 18 months of age (Figs. 4, 5). Figure 6 shows this progressive RGC loss in representative retinas from both strains from ages 3 to 18 months. As can be readily seen, RGC loss in C57 animals was diffusely distributed. In contrast, RGC loss in the DBA strain had a significant focal pattern (Fig. 6) manifested by large areas of retina with few (<100) or even no RGCs in frames that are clustered together, causing the appearance of a patch with severe loss of RGCs. Figures 7, 8, and 9 show retinal density maps for all the imaged retinas from DBA and C57 mice at 3, 15, and 18 months of age, respectively. The large areas of cell loss (patches) are indicated by asterisks on the RGC density maps of DBA mice in Figures 8 and 9. The counts show that RGC loss was variable at a given age in both strains but significantly more in the DBA strain. For example, one of the five 18-month DBA retinas imaged in Figure 9 maintained an almost normal number of RGCs, despite the age of the animal.

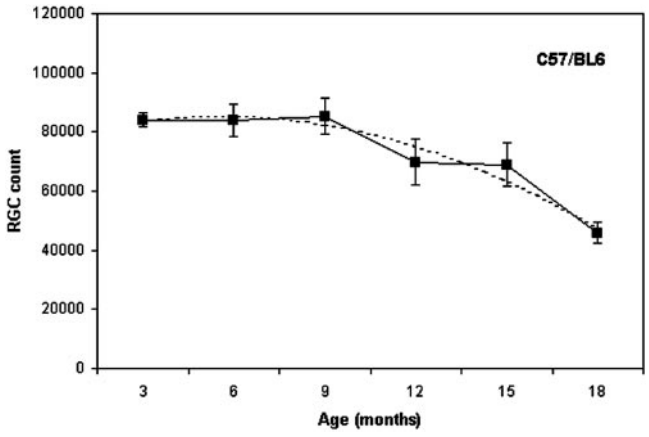

FIGURE 4. RGC counts (mean ± SEM) in C57/BL6 mice from 3 to 18 months of age (five eyes per time point). *Dotted line*: best-fitted decay curve to all the individual counts ($R^2 = 0.55$).

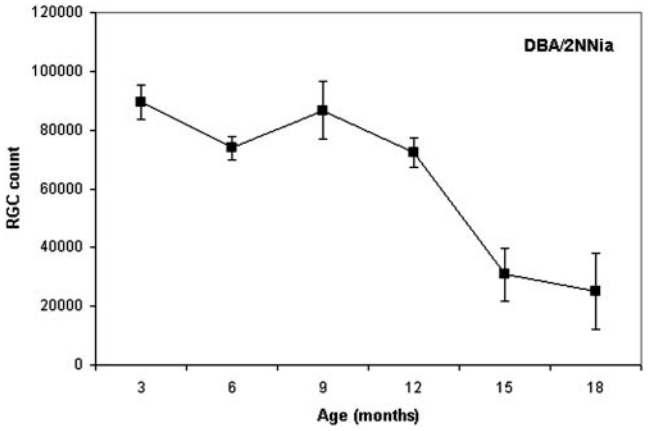

FIGURE 5. RGC counts (mean ± SEM) in DBA/2NNia mice from 3 to 18 months of age (five eyes per time point).

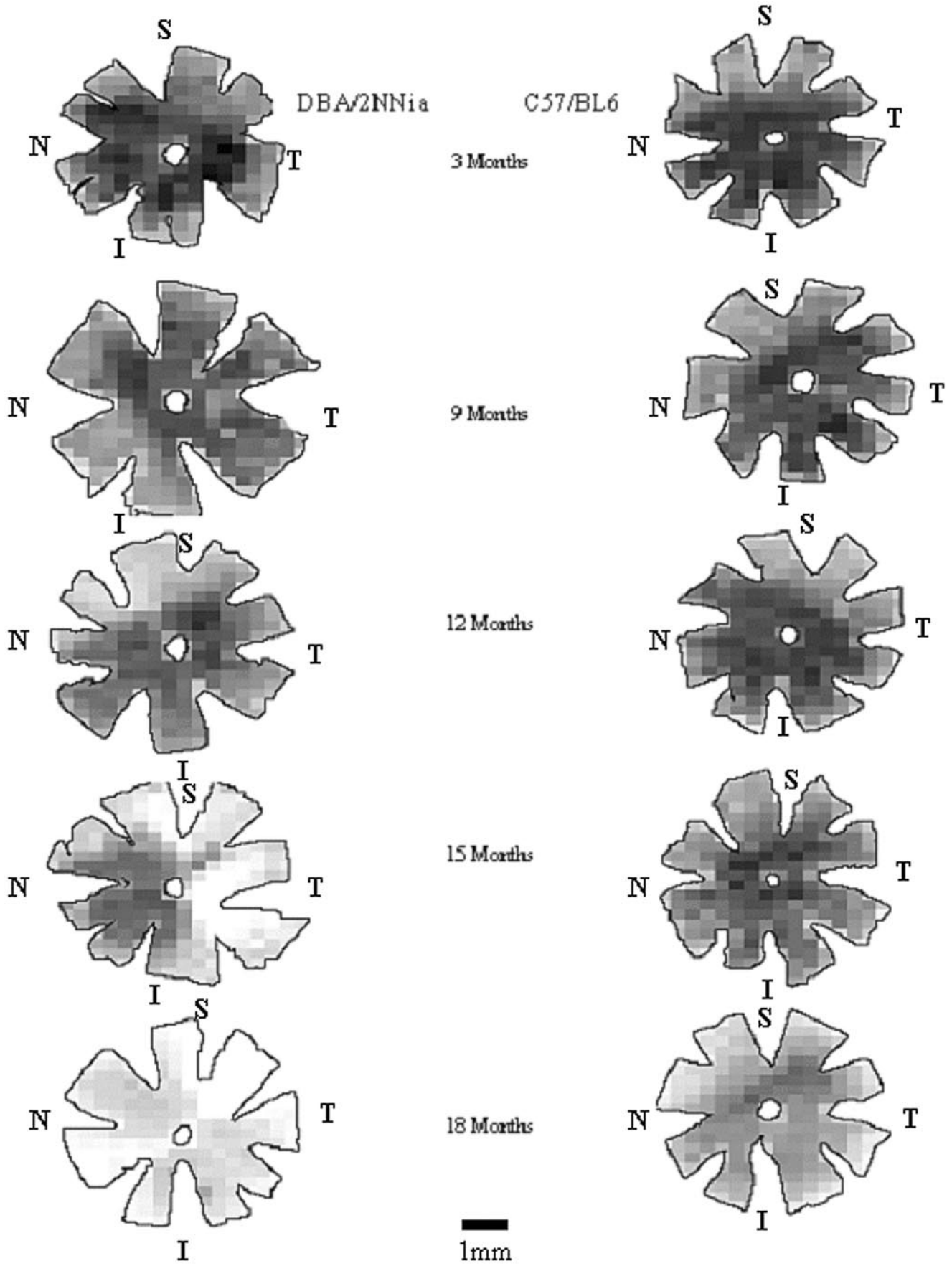

FIGURE 6. Representative retinal density maps from eyes of both C57 and DBA/2 animals from 3 to 18 months of age. To aid visual inspection, all retinas have been placed with the nasal side toward the *left*. N, nasal; T, temporal; S, superior; I, inferior. *Black*: highest RGC density.

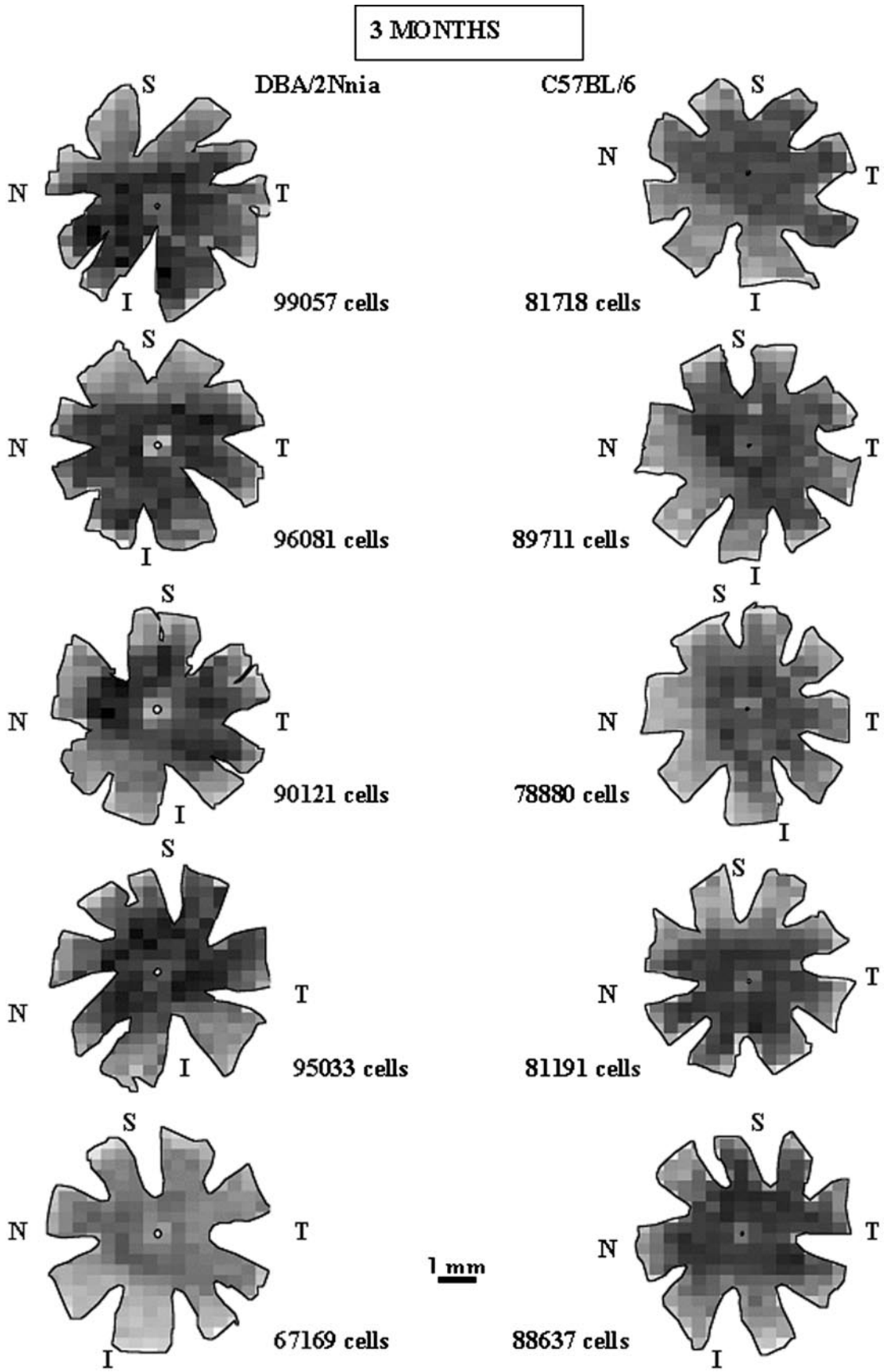

FIGURE 7. Retinal density maps of all eyes analyzed from 3-month-old C57/BL6 and DBA/2NNia animals. Abbreviations and orientation are as described in Figure 6.

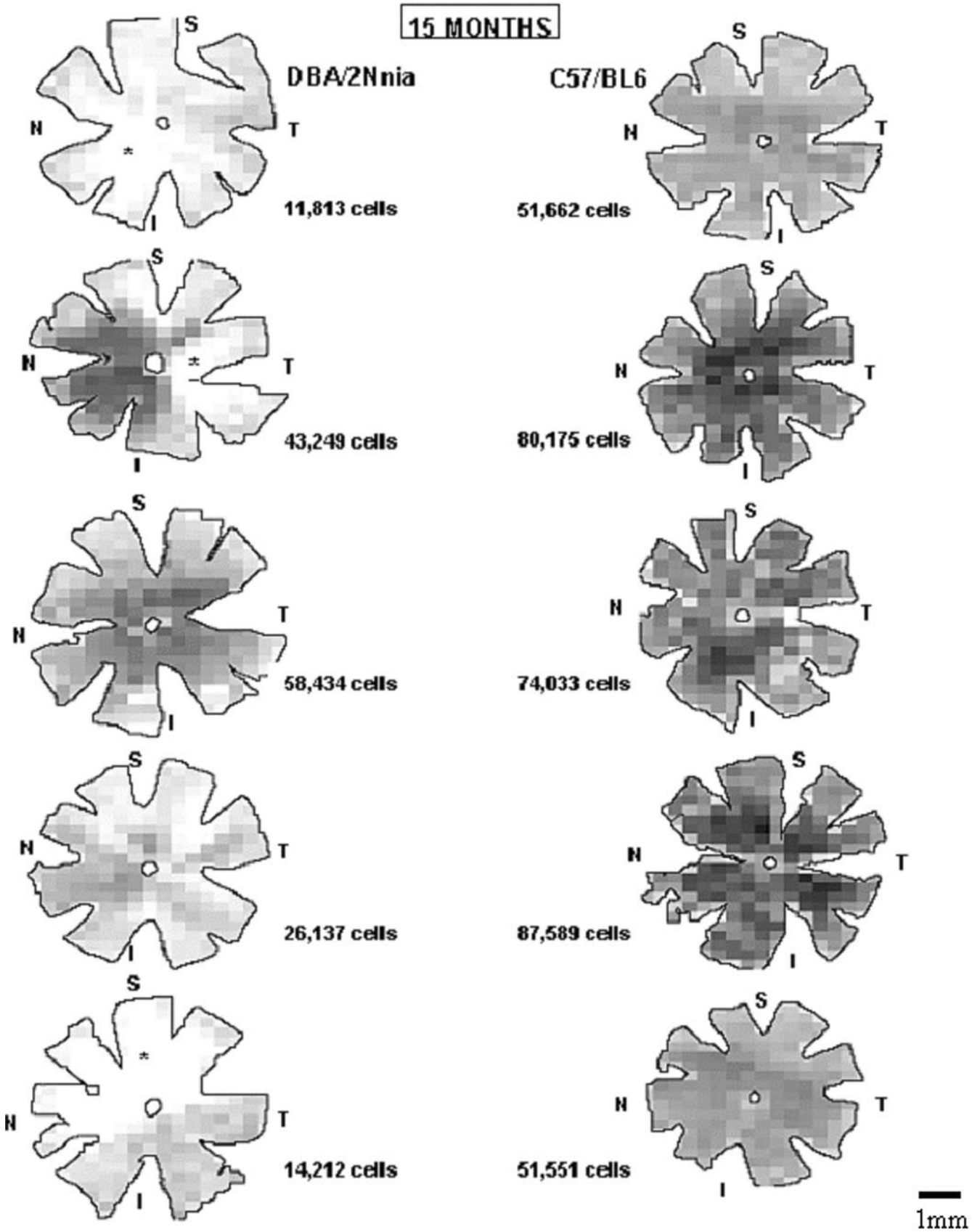

FIGURE 8. Retinal density maps of all eyes analyzed from 15-month-old C57/BL6 and DBA/2NNia animals. Numbers are the RGC counts in each eye. Abbreviations and orientation are as described in Figure 6.

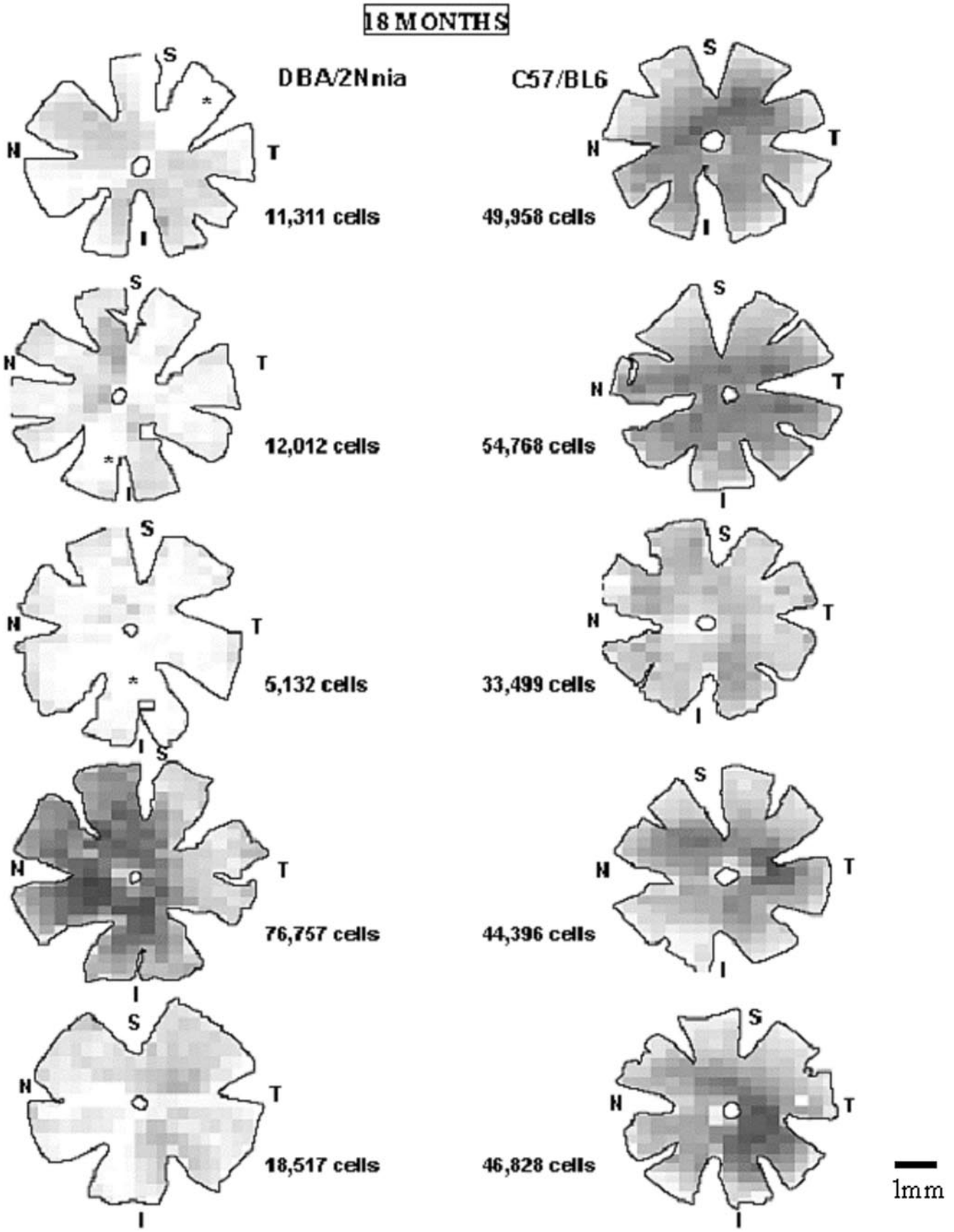

FIGURE 9. Retinal density maps of all eyes analyzed from 18-month-old C57/BL6 and DBA/2NNia animals. Numbers are the RGC counts in each eye. Abbreviations and orientation are as described in Figure 6.

Similarly, two of the five C57 retinas in Figure 8 showed significant loss of RGCs at 15 months.

Density Distribution in Mouse Retinas

To determine more precisely the pattern of RGC loss, we performed a distribution analysis of cell densities among the approximately 1200 frames combined from the images of the five retinas in each age group. The density range, starting from 1050 RGC/mm^2 or less, was binned in increments of 280 cells/mm^2 and the percent distribution of frames into these bins plotted in Figure 10. Figure 10A shows a similar distribution of RGC densities in 12-month-old C57 and DBA mouse retinas, similar to the distributions in 3-, 6-, and 9-month-old mice (data not shown). By 15 months of age, there was an overall shift in the distribution to lower cell densities with a particularly large increase in the proportion of frames of the lowest density (1050 RGC/mm^2 or fewer) to approximately 45% in DBA compared with the 6% low-density frames in C57 retinas (Fig. 10B). The downward shift in density distribution continued in 18-month-old DBA mice, with the low-density frames increasing to almost 60% of the retinal area (Fig. 10C). However, when the C57 density distribution in Figures 10B and 10C were compared, the distribution curve also appeared to shift to lower densities with age—that is, between 15 and 18 months of age, when the greatest loss of total RGC in C57 retinas occurred (Fig. 4). This shift is illustrated in Figure 10D, which directly compares 15- and 18-month-old C57 retinas and confirms the age-related shift of the RGC population to lower densities.

Discussion

DBA mice are beginning to be used as a noninduced rodent glaucoma model for dissecting the molecular mechanisms involved in glaucoma pathophysiology[15] and for testing neuroprotective substances. However, before embarking on such studies it is essential to know the rate of progression of the disease and to determine which component of the RGC loss may be age-related and which is attributable to glaucoma.

RGCs are the innermost layer of neurons in the retina. They are the highest order of neurons responsible for relaying the information gathered by photosensitive cells to higher centers in the brain. In the rat and mouse, most of the of these neurons project to the superior colliculus.[16] Although sampling approaches have been used in the past to estimate the number of RGCs, a systematic investigation of the total RGC population and its spatial distribution with the progression of age has not been performed.

Retrograde RGC labeling with Fluorogold (Fluorochrome, Englewood, CO) is a well-established procedure.[17–19] The total RGC counts obtained in younger unaffected DBA and C57 mouse retinas 3 to 9 months of age are slightly higher than the estimates obtained from axon counts in the optic nerve of mice,[20,21] perhaps because previous studies used axon sampling methods to estimate the number of RGCs. Although counting the myelinated axons in the optic nerve is relatively simple, nonmyelinated axons are harder to recognize, and their number varies significantly, depending on the location of the sample. Nonmyelinated axons can comprise from 2% to 50% of the axons in the optic nerve, depending on the location of the section.[20] An alternative explanation could be that the animals in the present investigation, although having the same genetic background as those reported by Williams et al.,[20] can represent slightly divergent subpopulations if they originate from different breeding facilities, as has been reported by these investigators.

It has been suggested that use of retrograde tracers may underestimate the real number of RGCs, because Fluorogold transport to the RGC body may be slowed by retinal disease, high IOP, or the aging process. Although possible, it is unlikely that a significant number of the surviving DBA2/NNia RGCs were not labeled with Fluorogold because of blockage of retrograde dye transport. The published data supporting blockade of retrograde flow of larger molecules at the lamina cribrosa[22–25] concern retrograde protein transport. In contrast,

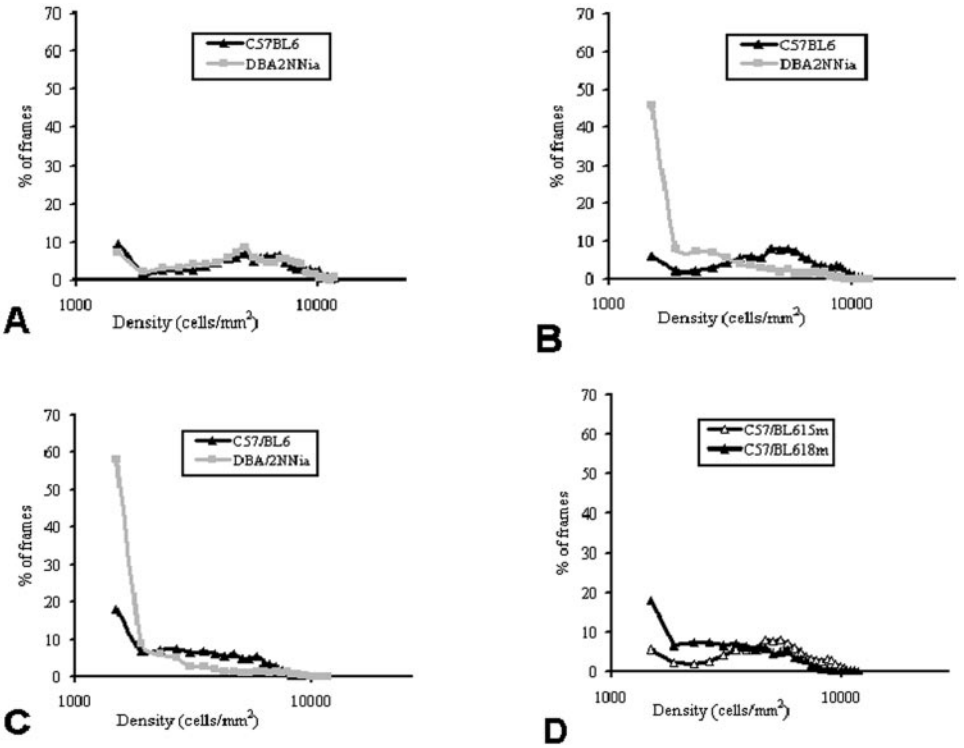

Figure 10. Distribution analysis of cell densities in all frames combined from the images of the five retinas in each age group (~1200 frames per group). Comparison is shown of RGC density distributions in C57 and DBA mouse retinas at (**A**) 12, (**B**) 15, and (**C**) 18 months of age and also (**D**) of RGC density distribution in C57 animals at 15 and 18 months of age.

Fluorogold is a small, highly charged cation that is very water soluble. It moves rapidly in optic nerve axons with initial RGC labeling occurring within 24 to 48 hours from the time of application to the superior colliculus. It is preferentially concentrated in the cell body of RGCs during the next 3 to 4 days, giving optimal images 5 to 7 days after application, without significant loss from cells within this time frame. Although Fluorogold is retrogradely transported by the vesicle system,[26] it should be pointed out that axonal transport in rodents is reduced but not eliminated by elevated IOP. Therefore, a slower dye transport would not explain the large areas of retina that have few or no RGCs in glaucomatous DBA/2 mice. The work of Johansson[27] shows that even with large molecules, retrograde transport in rats was slowed by only 20% to 25% when IOP was raised to 230% of the control eye. In DBA mice, mean IOP is less than twice the preglaucoma IOP.[1] Thus, even a 20% to 25% slowing in dye transport would be made up by the extra time we used for labeling.

Further evidence that use of Fluorogold does not overestimate RGC loss comes from the fact that although IOP elevation started at approximately 6 months of age (Fig. 3), RGC loss was not detected until after the 12th month of age. Our earlier study[3] documented that the retina of DBA/2NNia mice shows structural and electrophysiological changes starting at approximately 6 months of age. In addition, we now report that the total retinal area increased after the sixth month of age, probably as a result of high IOP and consequent scleral enlargement. However, RGC counts at 6, 9, and 12 months when IOP is elevated in a large number of eyes (Fig. 3), do not show a significant difference in total RGC numbers from the counts at 3 months. Thus, despite the occurrence of high IOP between 6 and 12 months of age, the number of RGCs does not decrease, suggesting that any effect of IOP on Fluorogold transport is not reflected in RGC counts obtained by our labeling procedure. IOP in the DBA mice returns to normal levels after the 12th month of age (Fig. 3, see also Ref. 1 and Pang I-H, et al. *IOVS* 1999;40:ARVO Abstract 3539). However pathologic RGC loss continued at a pace significantly faster than age-related RGC loss in C57 mice from 12 to 18 months of age. Finally, the pattern of labeling observed would be difficult to explain by axonal blockage of dye transport. There were some areas where RGC density was high, and all cells completely labeled; areas with fewer cells but with the surviving cells brightly labeled, and other areas with no RGCs, all in the same retina. These observations, taken together with those in the work of Sheldon et al.,[2] who used standard histologic methods to determine that RGC loss begins after 9 months of age in this strain, the foregoing discussion indicates that any underdetection of RGCs due to slowing of retrograde flow of Fluorogold would be small relative to the overall RGC loss. This small degree of underdetection (cell loss between 9 and 15 months of age is ~2.5% per week) could occur only during the 1 week of Fluorogold exposure and would not affect our ability to quantitate RGC loss accurately.

Although the speed of retrograde axonal transport in RGC axons might change with aging[28,29] or strain characteristics, such a change also would not affect RGC counting using the current methodology, because Fluorogold can be typically detected in the mouse retina as early as 24 to 48 hours after application to the superior colliculus and reaches a plateau of labeled cells by 4 to 5 days. The longer transport times that were used in the present study allowed RGC bodies to concentrate the dye further and thus improved imaging without causing significant leakage or transfer to other cells in the retina. In addition, differential Fluorogold uptake with age cannot explain the focal pattern of loss of RGCs observed in the DBA2/NNia mice nor the occasional retina with high RGC counts in aged DBA/2NNia animals (Fig. 9).

Age-related neuronal loss and decreases in the functional status of aging neurons have been proposed as alternative pathways responsible for the decline in mental function accompanying advanced age.[30] Multiple studies indicate a variable degree of neuronal loss according to the total cell population, animal species, and strain being studied.[6,8–11,31–36] It appears that an exponential decay of variable slope more adequately describes the results of various investigators as suggested previously.[11] However, despite such evidence, some investigators still assume a linear loss of RGCs with age.[37] Our results indicate that loss of RGCs most probably follows a second-order polynomial rate in aging C57/BL6 animals. RGC loss in the DBA strain appeared also to follow a second-order polynomial curve but at a different rate, thus sustaining the most significant loss during the period between 12 and 15 months with only small additional loss past that time point.

In addition, the topographical pattern of loss of RGCs appeared to be different among these two strains. DBA/2NNia animals showed a predominant focal pattern of RGC loss readily apparent in the retinal maps in Figures 8 and 9. In contrast, C57 mice showed a diffuse type of RGC loss at older ages, with patches devoid of cells rarely present in old C57 mouse retinas. The areas of patchy RGC loss in DBA retinas do not appear to localize in any one region of the retina. A comprehensive picture of this phenomenon is given by the density distributions in Figure 10. In 15- and 18-month-old DBA/2 mice, the low-density frames (<100 RGC per frame) make up 46% to 58% of the retinal area. The clustering of these low-density frames causes the observed areas of patchy loss. Such low-density frames also occur to some extent in old C57 mice when RGCs drop out from the lowest density peripheral areas, but they do not appear to cluster to form patches of RGC loss (Fig. 9). A diffuse dropout of RGCs may also be present in the DBA mice, as indicated by a downward shift in the overall cell density range shown in Figure 10. Because of the limitations of the methods used as well as the change in the total retinal area it is hard to judge whether this kind of RGC loss is qualitatively equivalent to the diffuse age-related RGC loss of the C57 strain. It is, however, interesting to observe that one of five retinas in the 18-month-old group of DBA animals in Figure 9 maintained a significantly higher number of RGCs and an almost normal cytoarchitecture, which we ascribe to the eye's not having had elevated IOP. This finding may indicate that nonpathologic age-related RGC loss proceeds at a slower pace in DBA mice than in C57 mice and that the RGC loss observed is mainly due to the glaucomatous disease process.

Earlier work on the anatomy of the mouse retina[38] has suggested that these animals do not have a well-defined macula as in primates and humans. Instead, RGC density seems to be higher in a paracentral area that lies temporal-superotemporal to the optic nerve head and is called the visual streak. In our experiments, the visual streak has not consistently localized temporally or superotemporally to the optic nerve head, both in rats[13] and in mice. This issue has been the topic of a letter to the editor of this Journal[39] regarding our previous publication,[13] and we have discussed possible explanations. It is partly for this reason that we did not undertake regional comparisons of the retinas of animals of different ages.

Previous studies in DBA/2 mice show that pathologic abnormalities in the anterior segment, thinning of nuclear and plexiform layers of the retina, decreases in ERG responses, and elevation of IOP all become evident at 6 to 7 months of age.[3] On the basis of these earlier findings we set the baseline age for the present study on RGC quantitation at 3 months, in anticipation of changes beginning at 6 months of age. However, the results clearly showed that although the total retinal area in-

creased at about the same time that IOP is known to increase,[1] the decline of RGC in DBA/2 mice began only at approximately 12 months of age. Thus, there was a lag time of approximately 6 months before anterior segment disease and an elevated IOP were manifested in the loss of RGCs. The thinning of the retina[3] and changes in the ERG[3,40] that also occur earlier, between 6 and 12 months of age, appear to be independent of RGC death and most likely represent a response of the retina to pressure stress and the need to cover larger area as the mouse eye enlarges.

Another interesting finding in DBA/2 mice is that the greatest RGC loss occurred between 12 and 15 months. However, the loss rate appeared to slow down after 15 months, as there was no statistically significant further loss by 18 months of age. This result may relate to the observations that in DBA/2J mice the IOP elevation began to return to the normal range at approximately 12 to 15 months of age,[41] as shown here also for the NNia substrain. This would remove the pressure stress on the retina and arrest the loss of RGCs. An alternative possibility is that approximately 20% to 25% of RGCs may be resistant to death by a pressure-induced mechanism.

Our findings also showed that there was a high degree of variability of RGC loss in DBA mice. This may relate to the mixed gender of the eyes studied (which was not recorded) and to a variable degree and length of time of IOP elevation among individual eyes, which was not determined in the same eyes in which RGC quantitation was performed because, at the time these studies commenced, there was no reliable noninvasive method to determine IOP in mouse eyes. Thus, drug studies on neuroprotection of RGC in DBA/2 mice require age selection and possibly gender selection and IOP history of the eyes. Age-related loss may contribute somewhat to the decrease in the number of RGCs. Because of the focal pattern of glaucomatous RGC loss, quantitation in such studies should involve counting the entire RGC population.

References

1. John SW, Smith RS, Savinova OV, et al. Essential iris atrophy, pigment dispersion, and glaucoma in DBA/2J mice. *Invest Ophthalmol Vis Sci*. 1998;39:951–962.
2. Sheldon WG, Warbritton AR, Bucci TJ, Turturro A. Glaucoma in food-restricted and ad libitum-fed DBA/2NNia mice. *Lab Anim Sci*. 1995;45:508–518.
3. Bayer AU, Neuhardt T, May AC, et al. Retinal morphology and ERG response in the DBA/2NNia mouse model of angle-closure glaucoma. *Invest Ophthalmol Vis Sci.* 2001;42:1258–1265.
4. Lynch S, Yanagi G, DelBono E, Wiggs JL. DNA sequence variants in the tyrosinase-related protein 1 (*TYRP1*) gene are not associated with human pigmentary glaucoma. *Mol Vis.* 2002;8:127–129.
5. Esiri MM, Hyman BT, Beyreuther K, Masters CL. Ageing and dementia. In: Graham D, Lantos L, eds. *Greenfield's Neuropathology.* London: Arnold; 1997;153–233.
6. Kemper TL, Moss MB, Rosene DL, Killiany RJ. Age-related neuronal loss in the nucleus centralis superior of the rhesus monkey. *Acta Neuropathol* (*Berl*). 1997;94:124–130.
7. Cavallotti C, Artico M, Pescosolido N, Feher J. Age-related changes in rat retina. *Jpn J Ophthalmol.* 2001;45:68–75.
8. Katz ML, Robison WG Jr. Evidence of cell loss from the rat retina during senescence. *Exp Eye Res.* 1986;42:293–304.
9. Shoji, M, Okada M, Ohta A, Higuchi K, Hosokawa M, Honda Y. A morphological and morphometrical study of the retina in aging SAM mice. *Ophthalmic Res.* 1998;30:172–179.
10. Weisse I. Changes in the aging rat retina. *Ophthalmic Res.* 1995; 27:(suppl 1):154–163.
11. Tatton WG, Greenwood CE, Verrier MC, Holland DP, Kwan MM, Biddle FE. Different rates of age-related loss for four murine monoaminergic neuronal populations. *Neurobiol Aging.* 1991;12:543–556.
12. Franklin K, Paxinos G. *The Mouse Brain in Stereotaxic Coordinates.* San Diego: Academic Press; 1977.
13. Danias J, Shen F, Goldblum D, et al. Cytoarchitecture of the retinal ganglion cells in the rat. *Invest Ophthalmol Vis Sci*. 2002;43:587–594.
14. Danias J, Kontiola AI, Filippopoulos T, Mittag T. Method for the noninvasive measurement of intraocular pressure in mice. *Invest Ophthalmol Vis Sci.* 2003;44:1138–1141.
15. Anderson MG, Smith RS, Hawes NL, et al. Mutations in genes encoding melanosomal proteins cause pigmentary glaucoma in DBA/2J mice. *Nat Genet.* 2002;30:81–85.
16. Jeffery G. Retinal ganglion cell death and terminal field retraction in the developing rodent visual system. *Dev Brain Res*. 1984;13: 81–96.
17. Manabe S, Lipton SA. Divergent NMDA signals leading to proapoptotic and antiapoptotic pathways in the rat retina. *Invest Ophthalmol Vis Sci*. 2003;44:385–392.
18. Vidal-Sanz M, Lafuente MP, Mayor S, de Imperial JM, Villegas-Perez MP. Retinal ganglion cell death induced by retinal ischemia. neuroprotective effects of two alpha-2 agonists. *Surv Ophthalmol.* 2001;45(suppl)3:S261–S267; discussion S273–276.
19. Levkovitch-Verbin H, Harris-Cerruti C, Groner Y, Wheeler LA, Schwartz M, Yoles E. RGC death in mice after optic nerve crush injury: oxidative stress and neuroprotection. *Invest Ophthalmol Vis Sci*. 2000;41:4169–4174.
20. Williams RW, Strom RC, Rice DS, Goldowitz D. Genetic and environmental control of variation in retinal ganglion cell number in mice. *J Neurosci.* 1996;16:7193–7205.
21. Williams RW, Strom RC, Goldowitz D. Natural variation in neuron number in mice is linked to a major quantitative trait locus on Chr 11. *J Neurosci.* 1998. 18:138–146.
22. Quigley HA, McKinnon SJ, Zack DJ, et al. Retrograde axonal transport of BDNF in retinal ganglion cells is blocked by acute IOP elevation in rats. *Invest Ophthalmol Vis Sci*. 2000;41:3460–3466.
23. Pease ME, McKinnon SJ, Quigley HA, Kerrigan-Baumrind LA, Zack DJ. Obstructed axonal transport of BDNF and its receptor TrkB in experimental glaucoma. *Invest Ophthalmol Vis Sci*. 2000;41:764–774.
24. Johansson JO. Influence of low IOP and low calcium on retrograde axoplasmic transport in rat optic nerve in vitro. *Exp Eye Res.* 1985;41:739–744.
25. Johansson JO. Inhibition of retrograde axoplasmic transport in rat optic nerve by increased IOP in vitro. *Invest Ophthalmol Vis Sci*. 1983;24:1552–1558.
26. Kobbert C, Apps R, Bechmann I, Lanciego JL, Mey J, Thanos S. Current concepts in neuroanatomical tracing. *Prog Neurobiol.* 2000;62:327–351.
27. Johansson JO. Inhibition and recovery of retrograde axoplasmic transport in rat optic nerve during and after elevated IOP in vivo. *Exp Eye Res.* 1988;46:223–227.
28. De Lacalle S, Cooper JD, Svendsen CN, Dunnett SB, Sofroniew MV. Reduced retrograde labelling with fluorescent tracer accompanies neuronal atrophy of basal forebrain cholinergic neurons in aged rats. *Neuroscience.* 1996;75:19–27.
29. Viancour TA, Kreiter NA. Vesicular fast axonal transport rates in young and old rat axons. *Brain Res*. 1993;628:209–217.
30. Anderton BH. Ageing of the brain. *Mech Ageing Dev.* 2002;123: 811–817.
31. Pugnaloni A, Pallotti F, Genova ML, et al. Histomorphometric studies in rat cerebral cortex: normal aging and cell loss. *Cell Mol Biol* (*Noisy-le-grand*). 1998;44:597–604.
32. Hof R, Bouras C, Perl DP, Sparks DL, Mehta N, Morrison JH. Age-related distribution of neuropathologic changes in the cerebral cortex of patients with Down's syndrome: quantitative regional analysis and comparison with Alzheimer's disease. *Arch Neurol*. 1995;52:379–391.
33. Merrill DA, Roberts JA, Tuszynski MH, Conservation of neuron number and size in entorhinal cortex layers II, III, and V/VI of aged primates. *J Comp Neurol.* 2000;422:396–401.
34. Merrill DA, Chiba AA, Tuszynski MH. Conservation of neuronal number and size in the entorhinal cortex of behaviorally characterized aged rats. *J Comp Neurol.* 2001;438:445–456.

35. Hequembourg S, Liberman MC. Spiral ligament pathology: a major aspect of age-related cochlear degeneration in C57BL/6 mice. *J Assoc Res Otolaryngol.* 2001;2:118–129.
36. Ransmayr G, Faucheux B, Nowakowski C, et al. Age-related changes of neuronal counts in the human pedunculopontine nucleus. *Neurosci Lett.* 2000;288:195–198.
37. Kawai SI, Vora S, Das S, Gachie E, Becker B, Neufeld AH. Modeling of risk factors for the degeneration of retinal ganglion cells after ischemia/reperfusion in rats: effects of age, caloric restriction, diabetes, pigmentation, and glaucoma. *FASEB J.* 2001;15:1285–1287.
38. Drager UC, Olsen JF. Ganglion cell distribution in the retina of the mouse. *Invest Ophthalmol Vis Sci*. 1981;20:285–293.
39. Reese BE. Rat retinal ganglion cell topography (E-Letter). *Invest Ophthalmol Vis Sci.* 2002.
40. Bayer AU, Brodie SE, Mittag T. Pilot study of pattern-electroretinographic changes in the DBA/2NNia mouse: animal model of congenital angle-closure glaucoma (in German). *Ophthalmologe.* 2001;98:248–252.
41. Anderson MG, Smith RS, Savinova OV, et al. Genetic modification of glaucoma associated phenotypes between AKXD-28/Ty and DBA/2J mice. *BMC Genet.* 2001;2:1.